

Effects of Array's Digital Beam Forming and Digital Polarization Synthesis Sequence on the Synthesis Results

Junrui Zhang¹, Lizhong Song¹, Qingfu Du², and Yao Chen²

¹School of Electronics and Information Engineering
Harbin Institute of Technology, Harbin, 150001, China
ivy Zhang@sdu.edu.cn, songlz@hit.edu.cn

²Institute of Space Sciences
Shandong University, Weihai, 264209, China
dqf@sdu.edu.cn, yaochen@sdu.edu.cn

Abstract — A polarized beamforming method of antenna array is addressed here. In this method, digital polarization synthesis (DPS) and digital beam forming (DBF) are processed separately in sequence. It synthesizes linearly-polarized antenna array into a circularly-polarized antenna whose main beam can scan in azimuth direction. The synthesis process and how the sequence affect the results are both expressed. It can be derived that with DPS-DBF (DPS first and DBF next), the beam is more smooth and has a better circular polarization in the main beam. This method can be used in solar radio observations and other systems that require wideband polarization measurements.

Index Terms — Antenna array, DBF, DPS.

I. INTRODUCTION

Polarization observation in the radio frequencies is critical to scientific studies in solar physics. Especially, circularly polarized signals are frequently used to infer the emission mechanism and the angle between the wave vector and the magnetic field. In order to meet the needs of the fine structure observation, the parabolic antenna or antenna arrays are always used to receive signals.

At meter or decameter wavelength, the parabolic is hard to construct, the antenna arrays are more commonly used. Then, due to the demand of circularly polarized observation, the polarization synthesis (PS) and beam forming (BF) are required. In some current solar radio observational systems, PS and BF are mostly implemented with analog devices (called APS and ABF), such as power combiner and phase shifter, they provide constant phase shift. Some systems uses hybrid digital and analog methods [6]. Some other systems use an identical coefficient matrix for both the PS and BF, such as the iterative least squares method [1,2,5], convex optimization [3,8], and other synthesizing methods [7,9,11]. However, according to the measuring methods

[10], measurements indicate that the axial ratio of these antenna sets (the cross LPDA and the hybrid coupler) is greater than 3 dB and reaches as high as 6 dB at some frequencies. That will lead to a low accuracy of polarization measurement, especially when dealing with wideband antennas.

A DPS method has been proposed for the cross-LPDA [4]. Here the DPS method is used in an array, and is carried out with the DBF in sequence separately in FPGA. The sequence of the two processes may affect the results, so whether and how it affects will be discussed in this work.

II. THE PROPOSED METHOD

The DPS and DBF methods both starts with the radiation patterns of the antennas. In this work, a three elements dual-polarized antenna array is used, each element is a cross-LPDA, which is constructed by two LPDAs placed horizontally and vertically.

Normally, the radiation pattern of an antenna in spherical polar coordinates can be expressed as follows:

$$E(\theta, \varphi) = \begin{bmatrix} E_{\theta} e^{jn_{\theta}(\theta, \varphi)} \\ E_{\varphi} e^{jn_{\varphi}(\theta, \varphi)} \end{bmatrix}. \quad (1)$$

The upper and lower terms in the brackets represent the electric component in the θ and φ directions (vertical and horizontal). In a dual-polarized antenna system, two antennas placed horizontally and vertically are generally called E_H and E_V , respectively:

$$E_H(\theta, \varphi) = \begin{bmatrix} E_{HV} e^{jn_{HV}(\theta, \varphi)} \\ E_{HH} e^{jn_{HH}(\theta, \varphi)} \end{bmatrix}, \quad (2)$$

$$E_V(\theta, \varphi) = \begin{bmatrix} E_{VV} e^{jn_{VV}(\theta, \varphi)} \\ E_{VH} e^{jn_{VH}(\theta, \varphi)} \end{bmatrix}. \quad (3)$$

According to the direction of the antenna, the two items in the brackets indicate the co-polarization

component (subscript HH (horizontal radiation component of the horizontal antenna) and VV (vertical radiation component of the vertical antenna)) or the cross-polarization component (subscript HV (vertical radiation component of the horizontal antenna) and VH (horizontal radiation component of the vertical antenna)), respectively. The radiation pattern is mainly decided by the excitation current and the antenna itself, and can be derived through simulation or measurement.

The three element dual-polarized antenna array then can be expressed as E_{H1} , E_{V1} , E_{H2} , E_{V2} , E_{H3} , E_{V3} . The

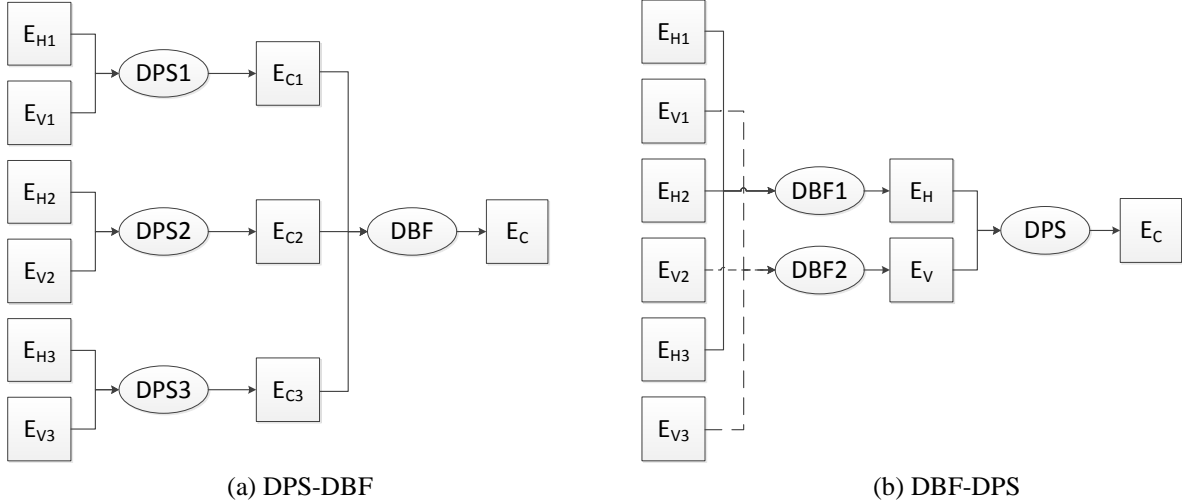


Fig. 1. Flowcharts of the two processes.

In the DPS process, the synthesizing coefficients are deduced from the simulated or measured data, and then, the coefficients are used for synthesis.

The synthesis process aims to find a complex factor ($k = \alpha + j\beta$, where α and β are real numbers) as a weighting in the vertical channel (E_V). Instead of the constant phase shift in APS, the complex factor is deduced from simulated or measured data. Then, the two linearly polarized antenna patterns are converted into left-handed and right-handed polarized antenna patterns by the following equation, where the parameters related to circularly polarized antennas are indicated by the subscript C:

$$\begin{bmatrix} E_{HH} e^{j\eta_{HH}(\theta, \varphi)} \\ E_{HV} e^{j\eta_{HV}(\theta, \varphi)} \end{bmatrix} + (\alpha + j\beta) \begin{bmatrix} E_{VH} e^{j\eta_{VH}(\theta, \varphi)} \\ E_{VV} e^{j\eta_{VV}(\theta, \varphi)} \end{bmatrix} = \begin{bmatrix} E_{CH} e^{j\eta_{CH}} \\ E_{CV} e^{j\eta_{CV}} \end{bmatrix}. \quad (4)$$

For the left-handed circular polarization,

$$E_{CH} = E_{CV}, \quad \eta_{CV} - \eta_{CH} = \frac{\pi}{2}. \quad (5)$$

For the right-handed circular polarization,

$$E_{CH} = E_{CV}, \quad \eta_{CV} - \eta_{CH} = -\frac{\pi}{2}. \quad (6)$$

proposed method deals with the DPS and DBF separately. There will be two kinds of processes, one is carry out DPS first and DBF next (named DPS-DBF), the other one is carry out DBF first and followed by DPS (named DBF-DPS), the flowcharts are shown in Fig. 1. With DPS-DBF, the three cross-LPDA are synthesized into three circularly polarized antennas first, and then they are beam formed. With DBF-DPS, the three horizontal polarized antennas and the three vertical polarized antennas are beam formed first, and then the two linearly polarized antennas are polarization synthesized.

The antenna parameters (E_{HH} , η_{HH} , E_{HV} , η_{HV} , E_{VH} , η_{VH} , E_{VV} and η_{VV}) can be obtained from either simulation or measurements, and E_{CH} , E_{CV} can be derived according to the law of energy conservation, and then, α and β expressed with the antenna parameters can be calculated by equation 4.

The DBF uses typical pattern synthesis method combining to the Taylor line source synthesis method. It synthesizes antenna patterns of the same polarization. Take horizontal antenna DPS as an example, the method can be expressed by equation (7). c_1 , c_2 , c_3 are three complex factors. Set $c_2 = 1$, the relative phase shift and weighting coefficients are represented as c_1 , c_3 , which can be calculated by the frequency, the element spacing, beam pointing direction and so on:

$$E_H = c_1 \times E_{1H} + c_2 \times E_{2H} + c_3 \times E_{3H}. \quad (7)$$

III. SIMULATION OF THE ARRAY

A 30~150MHz dual-polarized cross-LPDA (log periodic antenna) array is simulated and fabricated, as shown in Fig. 2. It is consist of three 16-dipole cross-LPDA. The length of the dipole ranges from 0.54m to

4.96m, the height of LPDA is about 5.3m. The interval of the antennas is 5m, and the reflector is 15.5m long and 5.15m wide. The S-parameters are shown in Fig. 3. It can

be seen that all the reflection coefficients are below -10 dB, and the isolations are all below -25 dB in the whole working band.

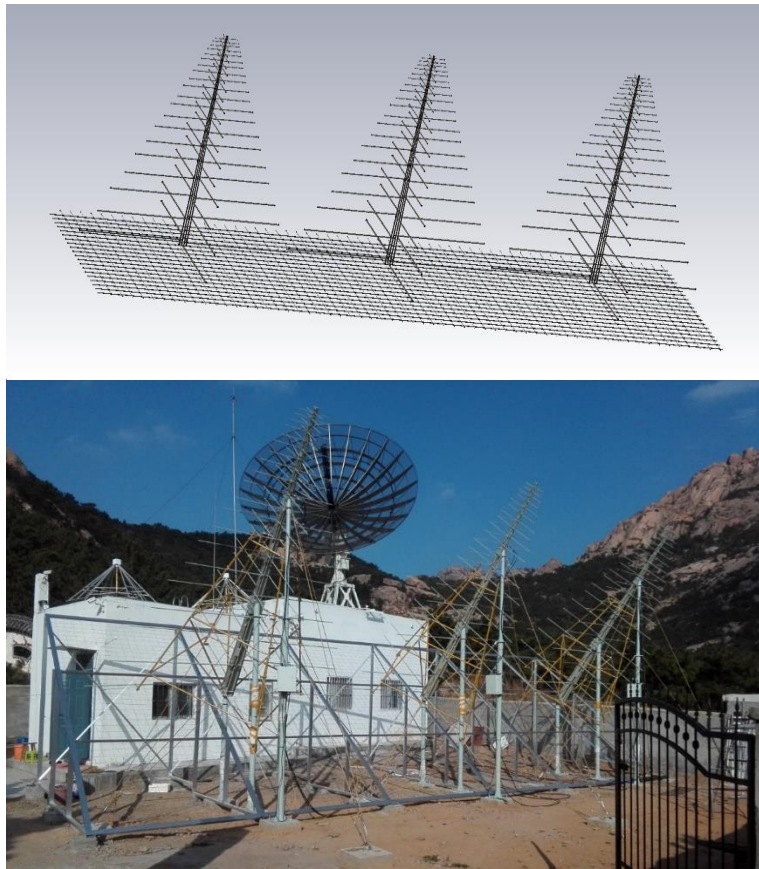


Fig. 2. The simulated model and the photo of the antenna array (three cross-LPDA with a flat reflector) installed at the Chashan solar radio station and operated by the Laboratory for Radio Technologies, Institute of Space Sciences at Shandong University.

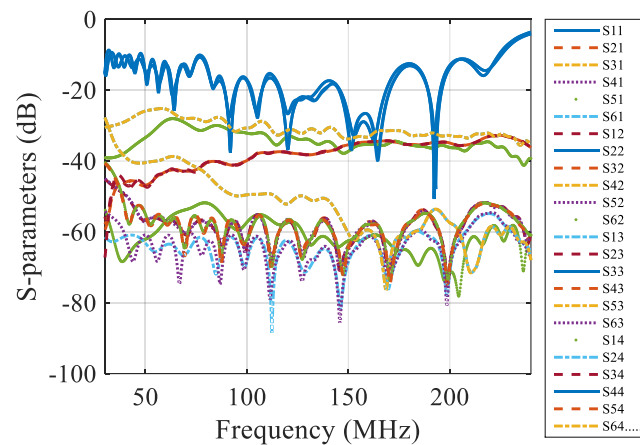


Fig. 3. S-parameters of the antenna array.

The 3dB beam width over the working frequency is shown in Fig. 4. It appears that the beam width is all above

90°. Hence, the array can scan in the range of -45°~45°. In a day, the sun passes about 15° per hour. When set 0°

points to the south (i.e., 12:00 noon), the array can be used to observe the sun from 9:00 to 15:00 every day.

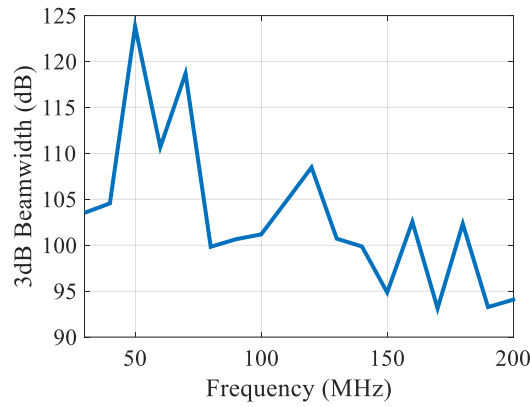


Fig. 4. 3dB beam width over frequency.

The simulated radiation patterns and the axial ratios of the three elements of the cross LPDA array are shown in Fig. 5. The results of the vertical ports are presented in Figs. 5 (a-b), and that of the horizontal ports are in (c-d). From Figs. 5 (a) and (c), it can be seen that the pattern of the three ports are almost the same, which shows good consistency. The maximum gains are both approximately

7.6 dB. From Figs. 5 (b) and (d), at the whole main beam (approximately $-45^{\circ}\sim 45^{\circ}$), the axial ratios of the three ports are both greater than 35 dB, indicating good linear polarizations. The vertical ones have higher purity of linear polarization, the axial ratios of which are all higher than 40 dB.

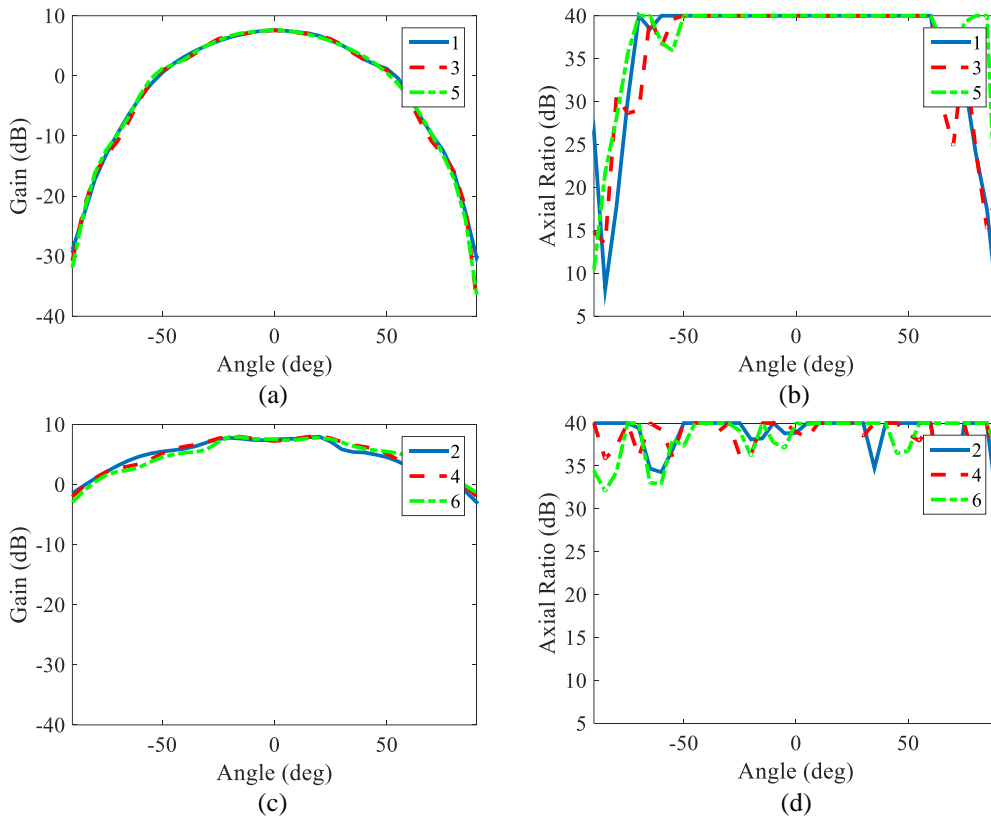


Fig. 5. The axial ratio and gain of the LPDA versus the angle (0° is the main radiation direction of the antenna) at a typical frequency of 90 MHz. Top panel: 3 vertical ports. Lower panel: 3 horizontal ports.

IV. ALGORITHM TEST AND COMPARISONS

Here we talk about the performance of the two kind of processes, DPS-DBF and DBF-DPS. The proposed method can be used in the main scan range, $0^\circ, \pm 10^\circ, \pm 20^\circ, \pm 30^\circ, \pm 40^\circ$ are tested. The simulated results show accordant consequences. Here we present 0° and 10° as an example to compare the two kinds of processes.

A. Pointing to 0°

a) DPS-DBF

In this case, DPS is processed first, the three sets of cross-LPDAs are separately polarization-synthesized to circular polarization at 0° , as in Fig. 1 (a). The results are

shown in Fig. 6. It shows that the axial ratio of the three sets are all 0 dB at 0° , and are lower than 3 dB in the main lobe. This indicates a good circular polarization performance. In addition, the maximum gain is 3 dB higher than the value before synthesis. This is due to the sum of energy of the two linearly polarized antennas.

Then, the three sets of synthesized circularly polarized antenna patterns are beam formed, the results are shown in Fig. 7. It can be seen that the axial ratio is still 0 dB at 0° , which shows pure circular polarization. Moreover, the axial ratio is relatively flat over the frequency. The maximum gain is about 20 dB, 3 dB bandwidth is about 10° , the gain of the first side beam is about 17 dB, which is 3 dB lower than the main beam.

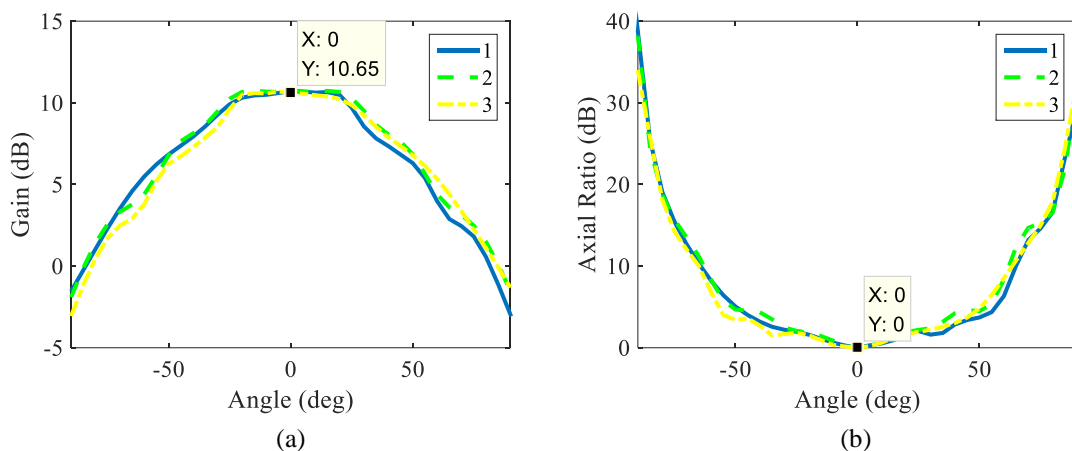


Fig. 6. The axial ratio and gain of the three sets of antenna elements after DPS at 0° .

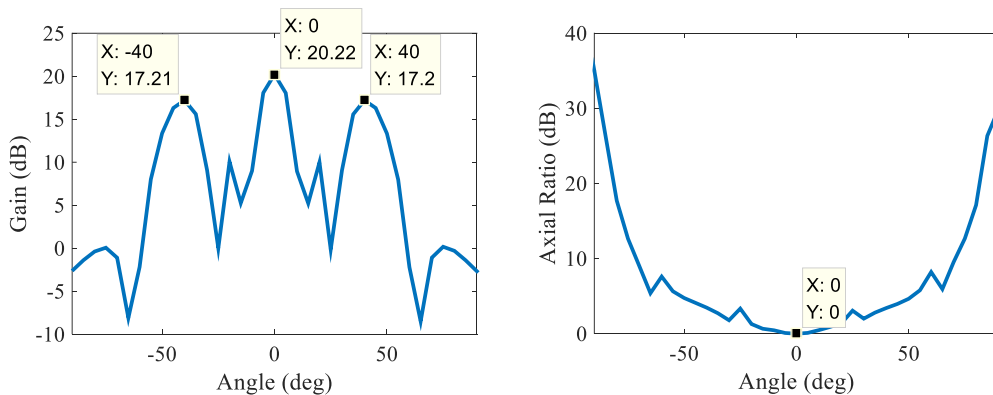


Fig. 7. The axial ratio and gain after DPS-DBF at 0° .

b) DBF-DPS

In this case, the three horizontal patterns and the three vertical patterns are first beam formed separately, as in Fig. 1 (b). The results are shown in Fig. 8. It shows

that the maximum gain is still appears at 0° , but there is a sharp drop next to the main lobe, and the entire pattern is very uneven. The maximum gain of the side beams are only 1 dB lower than that of the main beam in the two cases.

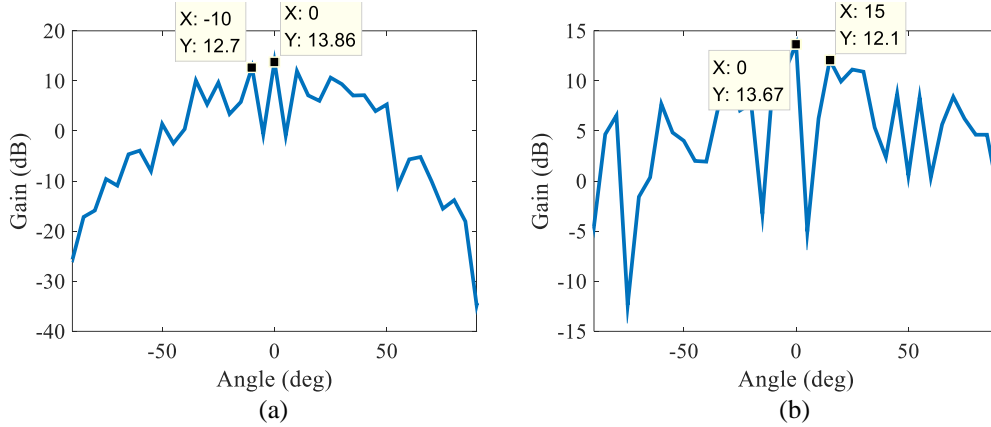


Fig. 8. Gain of the two patterns after DBF at 0°: (a) horizontal and (b) vertical.

On this basis, the two linearly polarized patterns are polarization synthesized to become a circularly polarized pattern. The axial ratio and gain are shown in Fig. 9. It can be seen that at 0°, the axial ratio is 0 dB, and the gain is 16.89 dB. The maximum gain of the side beam is

14.92, only 2 dB lower than the main beam, so further side-lobe suppression is required. In addition, the gain is not smooth and the main lobe is very narrow. Therefore, when the observation direction is slightly deviated, the observed results may have great errors.

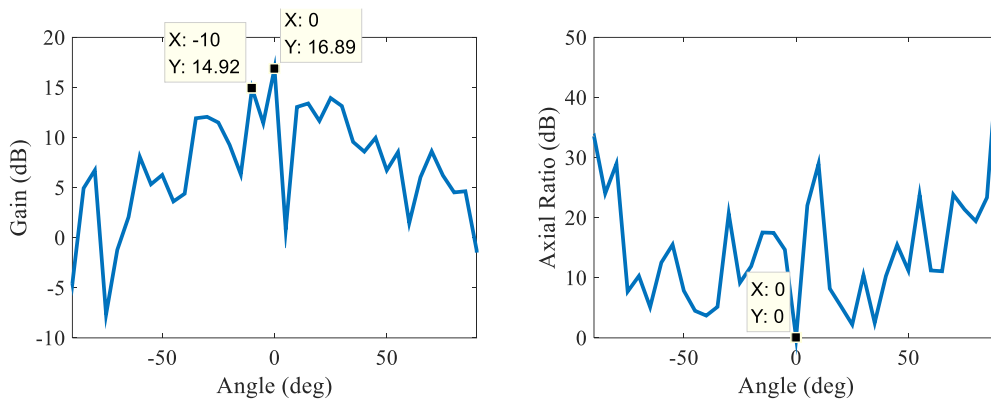


Fig. 9. The axial ratio and gain after DBF-DPS at 0°.

B. Pointing to 10°

This part talks about the scanning capability.

a) DPS-DBF

The three sets of cross-LPDA patterns are separately polarization-synthesized at 10°, as in Fig. 1 (a), and the results are shown in Fig. 10. It shows that maximum gain appears in 10°, the axial ratio of the three sets are all 0 dB at 10°, and it is lower than 3 dB in the main lobe. This indicates a good circular polarization performance.

Then, the three sets of patterns are beam formed, the results are shown in Fig. 11. It can be seen that the maximum gain is 19.87 dB, 3dB bandwidth is about 10°, the gain of the first side beam is 18.31 dB, which is 1.5 dB lower than the main beam. The axial ratio is still 0 dB at 10°, and is lower than 3 dB only in the main beam. That means the main beam is circularly polarized, and the side beam is not. Then, considering the axial ratio, when sun goes to 10°, the main beam is pointing to 10°, the side beam can receive few circularly polarized signals.

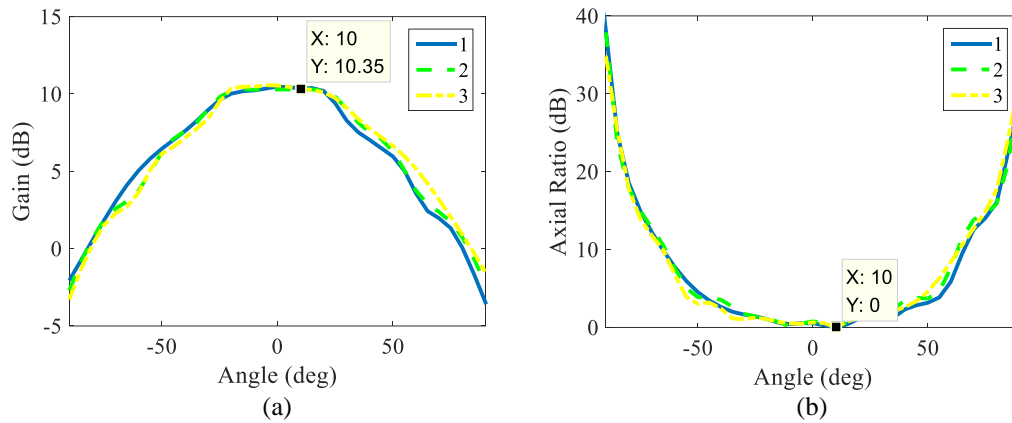


Fig. 10. The axial ratio and gain of the three synthesized antenna elements after DPS at 10°.

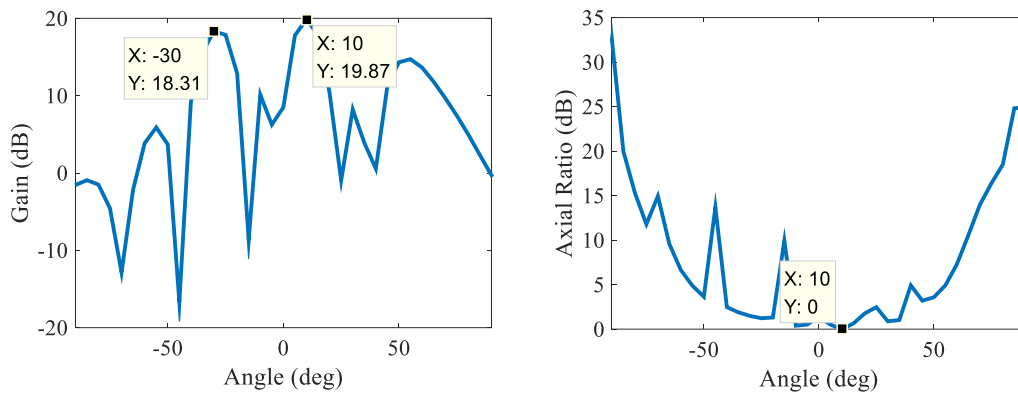


Fig. 11. The axial ratio and gain after DPS-DBF at 10°.

b) DBF-DPS

This time, the three horizontal patterns and the three vertical patterns are beam formed to 10° first, the results are shown in Fig. 12. It shows that the maximum gain

is still appears at 10°, but the first side lobe is almost as high as the main lobe, and the entire pattern is very uneven.

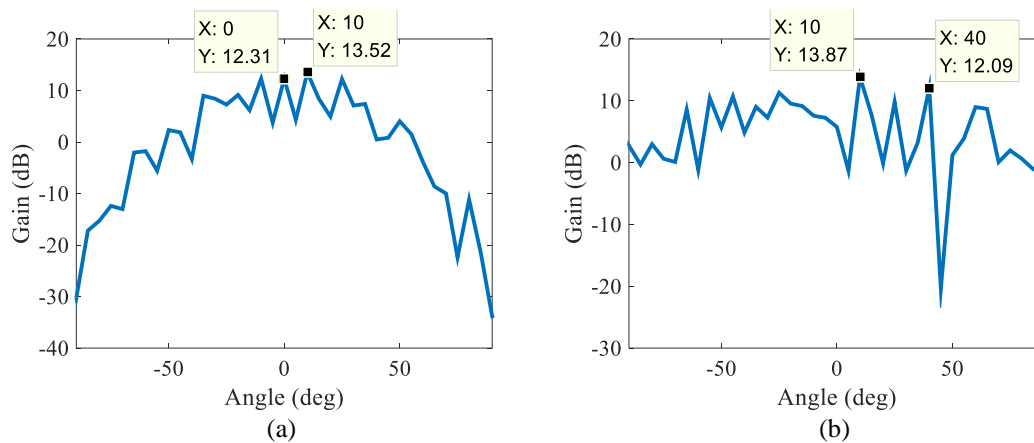
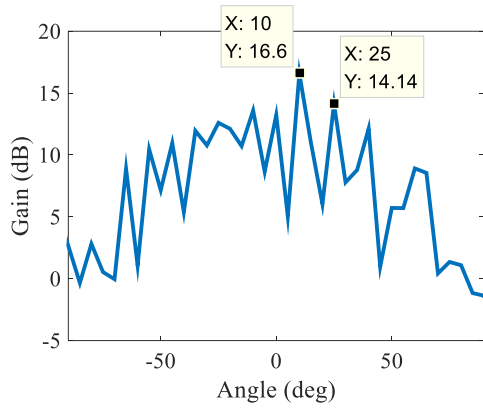


Fig. 12. Gain of the two patterns after DBF at 10°: (a) horizontal and (b) vertical.

Then, the two ports are polarization synthesized. The axial ratio and gain are shown in Fig. 13. It can be seen that at 10°, the axial ratio is 0 dB, and the gain is



the largest, which is 16.6 dB. The maximum gain of the side beam is 14.14 dB, only 2 dB lower than the main beam.

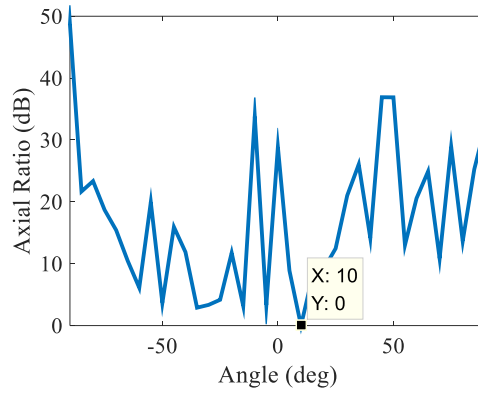


Fig. 13. The axial ratio and gain after DBF-DPS at 10°.

The results in 0° and 10° are compared in Table 1. With DPS-DBF, the total gain is larger, the axial ratio is smoother and circularly polarized in the main beam range. But with DBF-DPS, the axial ratio and gain both change greatly, so it can only be used in a very narrow range near the pointing point. In our work of solar observation, the DPS-DBF is more suitable.

Table 1: Comparison of the two processes

Pointing Direction	0°		10°	
	DPS-DBF	DBF-DPS	DPS-DBF	DBF-DPS
Maximum Gain (dB)	20.22	16.89	19.87	16.6
Maximum Gain of side beam (dB)	17.21	14.92	18.31	14.14

V. CONCLUSION

This paper discusses methods based on the demands of solar observation. They are used to synthesize linearly polarized antenna array into circularly polarized antenna. The results related to the sequences of DBF and DPS. It shows that with the DPS-DBF process, the synthesized antenna has a larger gain and better circular polarization at every directions.

These methods are also applicable to other fields which need polarized beam forming. When the measurement is carried out in real environments, the environmental interference and the inter-coupling between the antenna elements are also taken into account. It is easy to use when the measured errors can be neglected, and the axial ratio is reasonable. Even when the measurement is difficult to complete, we can first use the simulated data to deduce the synthesis parameters and then bring them into the system for

observation and calibration.

In addition, as the DPS and DBF are working as two independent computational processes, this method can also be used to synthesize two-dimensional arrays.

ACKNOWLEDGMENT

This work is sponsored by the National Natural Science Foundation of China (Grant No. 61571154) and the Field Foundation of the Ministry of Equipment Development of the Central Military Commission of China (Grant No. 6140415010305). The study at Shandong University was supported by the National Natural Science Foundation of China (11790303 (11790300), 41774180, and U1831101), and Shandong Provincial Natural Science Foundation, China (ZR201702100072).

REFERENCES

- [1] C. Dohmen, J. W. Odendaal, and J. Joubert, "Synthesis of conformal arrays with optimized polarization," *IEEE Transactions on Antennas & Propagation*, vol. 55, no. 10, pp. 2922-2925, 2007.
- [2] L. I. Vaskelainen, "Iterative least-squares synthesis methods for conformal array antennas with optimized polarization and frequency properties," *IEEE Transactions on Antennas & Propagation*, vol. 45, no. 7, p. 1179, 1997.
- [3] H. Leuret and S. Boyd, "Antenna array pattern synthesis via convex optimization," *IEEE Transactions on Signal Processing*, vol. 45, no. 3, p. 526, 1997.
- [4] J. R. Zhang, L. Z. Song, Q. F. Du, et al., "A wideband digital polarization synthesis method," *International Journal of RF and Microwave Computer-Aided Engineering*, e21411-, 2018.
- [5] B. M. Fabiani, et al., "Nonlinear constrained

beamforming algorithm for circularly-polarized phased arrays,” *IEEE Antennas and Wireless Propagation Letters*, vol. 17, pp. 1692-1696, Sept. 2018.

- [6] S. Foad and Y. Wei, “Hybrid digital and analog beamforming design for large-scale antenna arrays,” *IEEE Journal of Selected Topics in Signal Processing*, vol. 10, no. 3, pp. 501-513, Apr. 2016.
- [7] B. M. Fabiani and D. C. Nascimento, “Circularly-polarized antenna array for beam steering,” *IEEE International Symposium on Antennas & Propagation IEEE*, 2016.
- [8] B. Fuchs and J. J. Fuchs, “Optimal polarization synthesis of arbitrary arrays with focused power pattern,” *IEEE Transactions on Antennas & Propagation*, vol. 59, no. 12, pp. 4512-4519, 2011.
- [9] A. E. C. Tan and M. Y.W. Chia, “Beamforming and monopulse technique on sequentially-fed circularly-polarized ultra-wideband radar array,” *International Microwave Symposium Digest, IEEE*, 2009.
- [10] B. Y. Toh, R. Cahill, and V. F. Fusco, “Understanding and measuring circular polarization,” *IEEE Trans. Educ.*, vol. 46, no. 3, pp. 313-318, Aug. 2003.
- [11] S. Mubeen, A. M. Prasad, and A. J. Rani, “On the beam forming characteristics of linear array using nature inspired computing techniques,” *ACES Journal*, vol. 33, no. 2, Feb. 2018.



Junrui Zhang was born in 1982. She received her master degree from Southeast University in 2007, and is working towards the Ph.D. degree at Harbin Institute of Technology. Her research interests include antenna design, wireless electromagnetic wave propagation, and radar signal

processing.



Lizhong Song was born in 1975. He received master degree and Ph.D. degree from Harbin Institute of Technology in 2001 and 2005, respectively. He is a Professor and Doctoral Supervisor of Harbin Institute of Technology at Weihai. He focuses his academic interests on antenna design, wireless electromagnetic wave propagation, microwave technology and radar signal processing.



Qingfu Du received the master degree from Harbin Institute of Technology in 2007. He is an Assistant Professor of Shandong University (Weihai). His research interests mainly focus on sensors, high-precision instruments, industrial process automation and so on.



Yao Chen was born in 1975. He received his Ph.D. degree in Space Physics at USTC in 2004, and now is a Professor of Shandong University (Weihai). His primary research area is coronal dynamics, of particular interests are physical processes relevant to solar eruptions.